Image Anal Stereol 2001;20(Suppl 1): 556-560

DEPTH INTENSITY CORRECTION OF BIOFILM VOLUME DATA FROM CONFOCAL LASER SCANNING MICROSCOPES

KARSTEN RODENACKER[1], MARTINA HAUSNER[2], MARTIN KÜHN[2], STEFAN WUERTZ[2] AND SUMITRA PURKAYASTHA[3]

[1]GSF-National Research Center for Environment and Health, Institute of Biomathematics and Biometry, 85764 Neuherberg, Germany; [2]Institute for Water Quality Control and Waste Management, Technische Universität München, Germany; [3]GSF-IBB, Guest Scientist from Stat. Math. Unit, Indian Statistical Institute, Calcutta, India
e-mail: [redacted] karo13de@googlemail.com

ABSTRACT

Fluorescent signal intensities from confocal laser scanning microscopes (CLSM) suffer from several distortions inherent to the method. Namely, these are the decay of intensities with increasing depth by finite transparency of the media used, the effects of extinction of the examined objects, the bleaching of the fluorochrome and stray light at surfaces within the volume under research. Under certain assumptions the decay of intensities can be estimated and used for a partial depth intensity correction. This estimation of the approximated intensity decay function is described and its correction effect is outlined.
Volume and local distribution parameters of bacterial cultures marked by *fluorescent in situ hybridization* (FISH) are measured. Measurements with different corrections are compared with measurements of original data.

Keywords: biofilm, confocal microscopy, depth correction.

INTRODUCTION

Populations of bacteria in biofilms labelled by fluorescent oligonucleotide probes are digitized with a confocal laser scanning microscope (CLSM). These data are used to analyze the microbial community structure, to obtain information on the legalization of specific bacterial groups and to examine gene expression. In this study, a plasmid encoding a gene for the expression of the enhanced yellow fluorescent protein (EYFP) and FISH in combination with CLSM were used to determine in situ gene transfer frequencies in model bacterial biofilms. This information is urgently required for an in-depth understanding of the function and, more generally, the microbial ecology of biofilms (Hausner and Wuertz, 1999; Geisenberger *et al.*, 1999). Biofilms attached to a substratum in an experimental environment are analyzed by relating the different marked regions under consideration of the local bacterial density.

To obtain a reliable distinction between background and objects of interest, the segmentation of fluorescently-labelled bacteria, the original data obtained from CLSM have to be corrected. According to Ploem and Tanke (1987) and an early work of Rigaut and Vassy (1991) data and model-based correction improve the potential of 3-D measurements considerably. An correction scheme based on an approximated inversion of the CLSM transfer function was shown in Visser *et al.* (1991) by an iterative method and later improved by Roerdink and Bakker (1993) using the Fourier transform. In contrast to the relative large expense of computing time (Visser *et al.*, 1991; Roerdink and Bakker, 1993) we present a method to estimate approximately the intensity decay and use this function to correct either the measured fluorescent intensities or the segmentation threshold.

Segmented results are evaluated to obtain quantitative descriptions of volumetric, topological (and topographical) properties. Measurements are performed on different compartments of the components under research. Growth form as well as interaction of components can be quantitatively described. Classical measurements of volume and intensity (shape, distribution) and distance-dependent interaction measurements using methods from mathematical morphology are performed.

MATERIAL

The hybridized biofilm was automatically scanned with a Zeiss LSM410 CLSM (Kühn *et al.*, 1998). In each case, 9 vertical stacks of images (xy-sections, 512^2 pixels) were collected with 60 images (slices) per stack for the a biofilm using a 40x 1.3 NA oil immersion objective. The voxel size is $0.25 \times 0.25 \times 1.0(\mu m)^3$, hence one stack or volume block covers about 1 million $(\mu m)^3$.

Labelled cells were detected as follows: Recipients: 633 nm (excitation), 665 nm (emission); YFP-expressing cells: 488 nm (excitation), 525-540 nm (emission); transconjugants: probe-positive EYFP-expressing cells which were detected by co-localization (emission in both the 525-540 nm and >665 nm ranges). The relatively weak intensity signals have to be detected, displayed (Rodenacker *et al.*, 1997) and measured (Rodenacker *et al.*, 2000). The decay of intensities in depth is a major artifact for erroneous segmentation by intensity thresholds and succeeding measurements.

METHODS

ASSUMPTIONS

To estimate the intensity decay function (IDF) several model assumptions have to be considered. The following list is normally not fulfilled but helpful for the evaluation and model design: *(i)* homogeneity of medium in depth, *(ii)* independence of emission on depth, *(iii)* transparency of stained objects in depth, *(iv)* truncated emission values during digitization, *(v)* constant background noise intensity in depth and *(vi)* sufficiently distributed emitting material in depth.

These assumptions serve for simplification of the estimation of the correction function as well as for the correction itself. Critical are the assumptions *(i)*, *(ii)* and naturally *(vi)*. They are crucial for the estimation of the decay function. Using different data from FISH-labelled prostate tumors the decay could be nicely demonstrated by Purkayastha (2000). An exponential model of decay allowed a satisfying partial correction of depth influences. This method is extended and used to calculate the decay function by log-linear fitting. Main problem is the estimation of initial decay or loss based on the measured emission intensities.

OBSERVATIONS AND PHYSICAL PROPERTIES

Extinction of light caused by the surrounding medium - The decay caused by the medium has to be exponential. Let δ be the optical density of the medium per slice, Q the quantum efficiency of the fluorochromes, T_0 the excitation light at depth 0 (surface), $T_1(t)$ the excitation light at object location of depth t (see Fig. 1a), T_1' the emitted light at object location caused by excitation light T_1 and T_2' the measured emitted light at the surface ($t = 0$):

$$-\log\frac{T_1(t)}{T_0} \approx \delta t; \quad -\log\frac{T_2'}{T_1'(t)} \approx \delta t; \quad T_1' = QT_1 \quad \Rightarrow \quad T_2' \approx QT_0 e^{-2\delta t}\,. \tag{1}$$

Extinction of light by occlusion (shadowing) - The extinction by shadowing (see Fig. 1a) cannot be modelled theoretically. The measure of influences is strongly related to the amount of distributed material, its optical density or absorption respectively. We have examples with a 100% loss below (behind) certain objects. Of course in this case every correction approach will fail.

Intensity loss by bleaching - Assuming an image collection process starting at depth 0 and going down one (optical) section by one, the deepest sections are exposed to the excitation light for the longest period of time before their emission is measured. Depending on the sensitivity of the fluorochromes, a certain amount of bleaching and hence reduction of the quantum efficiency will occur.

Detector noise - When observing the distribution of the intensities of the interactively selected background of the data it can be deduced that background noise is independent on depth (Purkayastha, 2000).

CALCULATIONS

The depth histogram - We call the set of frequency distributions per depth the *depth histogram*, represented by a [*depth* × *intensity classes*] array. For visualization and possible insight this array can be displayed like an image where the x-coordinate represents the depth (slice #, e.g. $0 \cdots 59$), the y-coordinate the intensity class (e.g. $0 \cdots 255$, bin size 1) and the brightness (grey value) the frequency (white, e.g. ≈ 2000) (see Fig. 1b). Typically, the depth histogram is generated as an accumulated histogram from all volume stacks to obtain a better statistical representation.

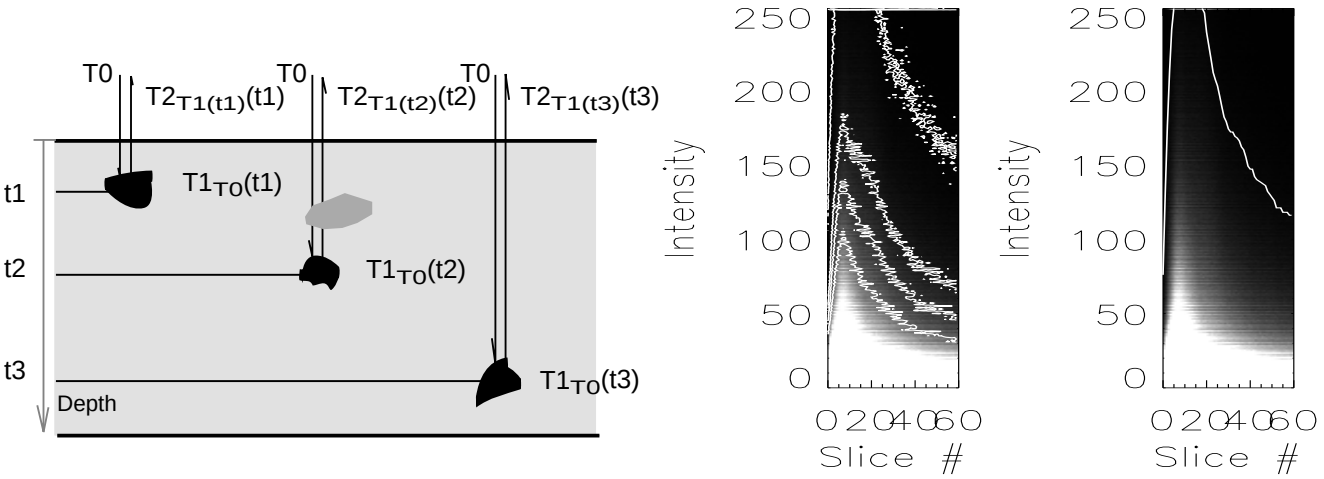

(a) (b)

Fig. 1. *(a) Illustration of depth influence to excitation and emission light; T0 excitation light at the surface, T1 excitation light at object depth, T2 emission light at surface, b) Image representation of depth histogram from recipients with* frequency thresholds *less than (20, 200, 400, 800) marked by contours (left, see text) and the 99.9% percentile as first estimate of the IDF (right).*

The intensity decay function *IDF* - The IDF should monotonously decrease under the assumptions stated above. A first approach to find some possible points of the function is the usage of very small quantiles of the depth histogram. A first estimate for the IDF is the 99.9% percentile per depth, shown in Fig. 1b. Of course this can only be a lower limit of the true IDF.

The 99.9% percentile for the two fluorochromes is shown in Fig. 2a. Since any intensity decay has to be monotone, the increasing intensity in the first slices is caused by the lack of adequate material. This is illustrated in Fig. 2b by a vertical section through a block. This region is represented by a constant function from depth 0 up to the location of the maximum (in Fig. 2a at section # 20). The rest is logarithmically transformed, fitted by the `ladfit` procedure from *IDL*. This is a linear fit using a ”robust” least absolute deviation method and transformed back. This corresponds to the theoretical decay of intensities by depth (see Sec. 3.2), the findings in Rigaut and Vassy (1991) and Purkayastha (2000).

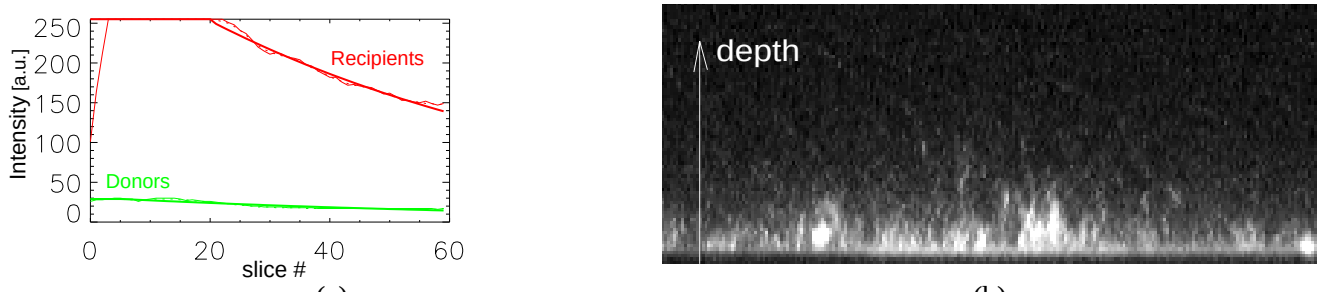

(a) (b)

Fig. 2. *(a) Decay of intensity in depth, estimated from nine volume blocks for two different fluorochromes, (b) Vertical volume section (summed up from several sections to show a more representative, however blurred profile). The depth is vertically strongly enlarged.*

A second method of estimation of the IDF is also used by applying a set of quantile values, calculating a set of functions and defining the final IDF by the mean of the exponential factor of the fits of this set of functions. This method allows a finer tuning of the influences of material distribution in depth.

The correction function - The final IDF(Fig. 2a) is used to calculate the correction function (Fig. 3a)

$$corr(t) = \frac{\max_{\forall t}(IDF(t))}{IDF(t)}, \tag{2}$$

which is applied by multiplication to the measured intensities.

IMPLEMENTATION

The programs are written in IDL (Interactive Data Language, Research System Inc., Boulder, USA). Calculations were performed on different platforms, mostly PC's and Unix workstations. A whole package of routines (`depth_...`) covering many aspects of depth histogram manipulation from generation through transformation to display and interactive access is implemented. The package is not limited to the reported approach and is used for many other applications with 3- and higher dimensional data with similar problems like magnetic resonance image data (MRI) as well as functional MRI (fMRI).

RESULTS

With one fixed threshold all measurements on the original and the corrected data were performed. The threshold was in this case interactively selected by the biologist according to the biochemical and morphological properties of the probes used. For nine volume blocks (stacks) the measured volumes of recipients and donors are displayed per depth (Fig. 3b). The dashed lines show the volumes of the original data and the solid lines the volumes of the corrected data. The corresponding correction functions are shown in Fig. 3a. The amount of labelled biomass reaches a maximum at about $10\mu m$ (10 slices by $1\mu m$) distance from the substrate at depth 0 and decreases than to about half of the maximum for recipients and to a quarter of the maximum for donors. For recipients the measurements from corrected data correspond with visual observation. For donors the slight increase of volume at the end of the measurement depth feeds suspicion for over-correction. However the donor volume is to small for visual inspection and comparison.

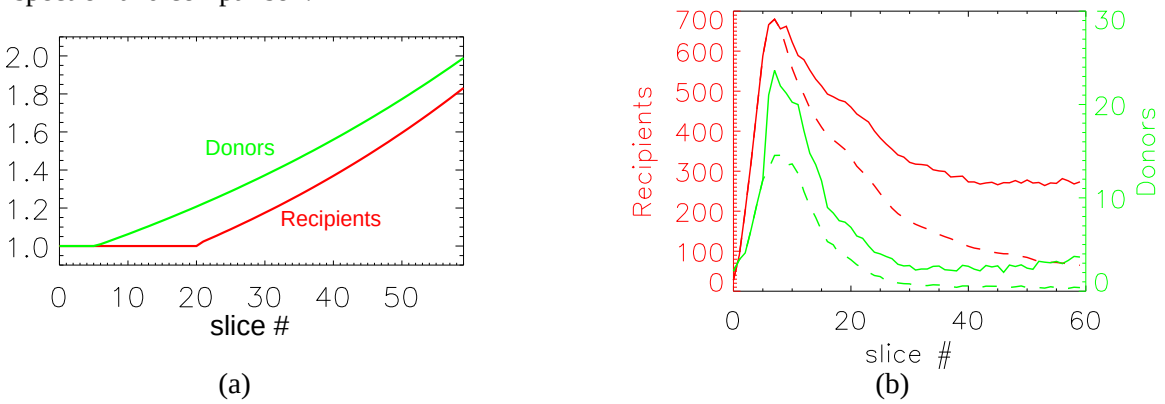

Fig. 3. *(a) Multiplicative correction function for two different fluorochromes, (b) Mean volumes per depth from 9 stacks for two different fluorochromes; solid line corrected data, dashed line original data.*

For control and comparison of the methods applied the correction scheme by Visser *et al.* (1991); Roerdink and Bakker (1993) was applied. Although there was no hint given for adjustment of the necessary parameters, the correction performed delivered for our material similar characteristics. The magnitude of this Roerdink and Bakker (1993) correction was highly dependent on the chosen parameters.

DISCUSSION

The proposed correction function can only correct partial influences of depth. Several assumptions served for the design of this functions are only partly fulfilled. Critical assumptions are the homogeneity of medium, the assumed sufficient distribution of labelled material and the constancy of emission in depth. The first assumption can become questionable if EPS is present. The second is possibly not fulfilled for the very sparsely distributed donors and the third assumption considers bacteria as independent on depth which is true for certain types of biofilms but probably not for all. At least the correction by Visser *et al.* (1991); Roerdink and Bakker (1993) showed that for the data used our in terms of computing time very cheap correction method is acceptable and comprehensible.

In the case of donors data correction the found function is similar to the one found for recipients. However the fluorochrome EYFP is a very stable one with very little amount of bleaching. Combined with the very sparsely distributed bacteria the assumptions might not be fulfilled. For verification of the correction further experiments with varying amounts of grown material have to be performed.

The data used are biofilms grown in a flow channel which can be mounted on the CLSM. The volume data were gathered without any fixation. Up to now there is for this type of experiments no procedure known to validate the measurements on corrected data beside mere plausibility. Beside the necessary enlargement of the data base additional work has to be directed to the identification and reduction of the noise by (non-)linear smoothing.

ACKNOWLEDGEMENTS

This work was funded in parts by DFG:SFB411, BMBF:IB INI-027-96, Germany and ICMR, India.

REFERENCES

Geisenberger O, Ammendola A, Christensen BB, Molin S, Schleifer KH, Eberl L (1999). Monitoring conjugal transfer of plasmid RP4 in activated sludge and in situ identification of the transconjugants. FEMS Microbiol Lett 174:9-17.

Hausner M, Wuertz S (1990). High initial frequencies of conjugation in biofilms as determined by quantitative in situ analysis. Appl Environ Microbiol 65(8):3710-3.

Kühn M, Hausner M, Bungartz HJ, Wagner M, Wilderer PA, Wuertz S (1998). Automated confocal laser scanning microscopy and semi-automated image processing for the analysis of biofilms. Appl Environ Microbiol 64:4115-27.

Ploem JS and Tanke HJ (1987). Introduction to fluorescence microscopy, Vol 10 of Microscopy Handbooks. Oxford University Press, Royal Microscopical Society.

Purkayastha S (2000). Two examples of biomedical imaging. Work report 00-08, GSF-IBB. `http://www.gsf.de/ibb/preprints/2000/pp00-08.ps`

Rigaut JP, Vassy J (1991). High-resolution three-dimensional images from confocal scanning laser microscopy. Anal Quant Cytol Histol 14(4):223-32.

Rodenacker K, Aubele M, Hutzler P, Umesh Adiga PS (1997). Groping for quantitative digital 3-d image analysis: An approach to quantitative fluorescence in situ hybridization in thick tissue sections of prostate carcinoma. Anal Cell Pathol 15:19-29.

Rodenacker K, Brühl A, Hausner M, Kühn M, Liebscher V, Wagner M, Winkler G, Wuertz S (2000). Quantification of biofilms in multi-spectral digital volumes from confocal laser-scanning microscopes. Image Anal Stereol 19(1):39-43.

Roerdink JBTM, Bakker M (1993). An FFT-based method for attenuation correction in fluorescence confocal microscopy. J Microsc 169(1):3-14.

Visser TD, Groen FCA, Brakenhoff GJ (1991). Absorption and scattering correction in fluorescence confocal microscopy. J Microsc 163(2):189-200.